

Pattern Replication by Confined Dewetting

Stephan Harkema, Erik Schäffer,[†] Mihai D. Morariu, and Ullrich Steiner*

Department of Polymer Chemistry and Materials Science Center, University of Groningen, Nijenborgh 4, NL-9747 AG Groningen, The Netherlands

Received March 27, 2003. In Final Form: June 11, 2003

The dewetting of a polymer film in a confined geometry was employed in a pattern-replication process. The instability of dewetting films is pinned by a structured confining surface, thereby replicating its topographic pattern. Depending on the surface energy of the confining surface, two different replication mechanisms were found, leading to a choice of either a negative or a positive replication mechanism of a patterned plate.

1. Introduction

The conformation of liquids in a confined geometry differs compared to their behavior in large volumes. This is due to the dominance of the liquid's surface and interfacial tension over other body and surface forces at small (mesoscopic) length scales.¹ The relevant range in length is bounded by the capillary length $a = (2\gamma/\rho g)^{1/2}$, quantifying the balance between the surface energy γ and the gravitational acceleration g of the liquid with density ρ . The lower limit is given by molecular length scales, where the confinement of liquids can lead to a layering of the molecules,² a change in the freezing^{3,4} and glass transition temperatures,^{5,6} or a modified rheology.⁷ In the capillary regime, liquid morphologies are dominated by a minimization of the overall surface free energy. Because the interface between the liquid and a confining solid often has a lower energy per unit area compared to the liquid–air and the solid–air surfaces, this leads to liquid morphologies that are not observed for large volumes of liquids. Well-known examples include the capillary rise of a liquid in a narrow tube, the formation of a liquid bridge spanning two opposing finger tips, or the fact that large amounts of water are drawn into a granular material (e.g., sand), overcoming the gravitational counterforce.

A second aspect where the finite size of a liquid sample plays a role concerns the stability of thin films. While planar liquid films are intrinsically stable, they can be destabilized by a force that causes a negative disjoining pressure (i.e., a force tending to reduce the thickness of the film). For example, the dewetting of polymer films driven by a van der Waals pressure has been the subject of intensive research.^{8–14} Destabilizing van der Waals forces cause the amplification of a capillary mode with a

well-defined wavelength,^{15,16} giving rise to a characteristic spinodal surface pattern and eventually to a breakup of the films into an array of drops. A negative disjoining pressure was also predicted to arise from the confinement of acoustic modes.¹⁷

Here, we describe the interplay of these two confinement-induced effects: the spontaneous destabilization of a thin film and the capillary bridging of the resulting pattern in a structured slit pore. This interplay between dewetting and capillary bridging can be harnessed as a pattern-replication technique. If confined by a topographically structured surface, the undulatory mode of the film instability is pinned at the locations of smallest confinement. In the case of an apolar confining surface, this leads to a long-lived metastable conformation of the liquid that mirrors the topographic pattern of the confining surface.

While both the capillary condensation in a patterned slit pore^{18,19} and van der Waals driven dewetting in the presence of lateral heterogeneities^{20–22} were described before, our work differs from these earlier studies in two aspects. By using nonvolatile polymers, the formation of capillary bridges occurs exclusively via hydrodynamic flow rather than by transport through the gas phase (capillary condensation). As opposed to dewetting on structured substrates, the initial breakup of the film is only weakly affected by the presence of the confining surface and, therefore, by its lateral structure, which manifests itself mainly during the late stage of the film instability. Our study bears, on the other hand, resemblance to recent experiments, in which electric fields^{23,24} or temperature gradients^{25–27} were employed to destabilize thin polymer films, replicating topographic patterns with feature sizes

* Corresponding author. E-mail: u.steiner@chem.rug.nl.

[†] Present address: Max Planck Institute of Molecular Cell Biology and Genetics, D-01307 Dresden, Germany.

(1) Myshkis, A. D.; Babskii, V. G.; Kopachevskii, N. D.; Slobozhanin, L. A.; Tyuptsov, A. D. *Low-Gravity Fluid Mechanics*; Springer-Verlag: Berlin, 1987.

(2) Israelachvili, J. *Intermolecular and Surface Forces*; Academic Press: London, 1995.

(3) Granick, S. *Science* **1991**, *253*, 1374.

(4) Klein, J.; Kumacheva, E. *J. Chem. Phys.* **1998**, *108*, 6996.

(5) Reiter, G. *Europhys. Lett.* **1993**, *23*, 579.

(6) Keddie, J. L.; Jones, R. A. L.; Cory, R. A. *Europhys. Lett.* **1994**, *27*, 59.

(7) Israelachvili, J.; McGuiggan, P. M.; Homola, A. M. *Science* **1988**, *240*, 189.

(8) Reiter, G. *Phys. Rev. Lett.* **1992**, *68*, 75.

(9) Reiter, G. *Science* **1998**, *282*, 888.

(10) Jacobs, K.; Herminghaus, S.; Mecke, K. R. *Langmuir* **1998**, *14*, 965.

(11) Reiter, G.; Sharama, A.; Casoli, A.; David, M.-O.; Khanna, R.; Auroi, P. *Langmuir* **1999**, *15*, 2551.

(12) Reiter, G.; Khanna, R.; Sharma, A. *Phys. Rev. Lett.* **2000**, *85*, 1432.

(13) Khanna, R.; Sharma, A.; Reiter, G. *EPJdirect* **2000**, *E2*, 1.

(14) Seemann, R.; Herminghaus, S.; Jacobs, K.; *Phys. Rev. Lett.* **2001**, *86*, 5534.

(15) Vrij, A. *Discuss. Faraday Soc.* **1966**, *42*, 23.

(16) Brochard-Wyart, F.; Dailant, J. *Can. J. Phys.* **1990**, *68*, 1084.

(17) Schäffer, E.; Steiner, U. *Eur. Phys. J. E* **2002**, *8*, 347.

(18) Röcken, P.; Somoza, A.; Tarazona, P.; Findenegg, G. *J. Chem. Phys.* **1998**, *108*, 8689.

(19) Henderson, D. *Fundamentals of Inhomogeneous Fluids*; Marcel Dekker: New York, 1991.

(20) Kargupta, K.; Sharma, A. *Phys. Rev. Lett.* **2001**, *86*, 4536.

(21) Kargupta, K.; Sharma, A. *J. Colloid Interface Sci.* **2002**, *245*, 99.

(22) Kargupta, K.; Sharma, A. *Langmuir* **2002**, *18*, 1893.

(23) Schäffer, E.; Thurn-Albrecht, T.; Russell, T. P.; Steiner, U. *Nature* **2000**, *403*, 874.

(24) Schäffer, E.; Thurn-Albrecht, T.; Russell, T. P.; Steiner, U. *Europhys. Lett.* **2001**, *53*, 518.

(25) Schäffer, E.; Harkema, S.; Blossey, R.; Steiner, U. *Europhys. Lett.* **2002**, *60*, 255.

(26) Schäffer, E.; Harkema, S.; Roerdink, M.; Blossey, R.; Steiner, U. *Macromolecules* **2003**, *36*, 1645.

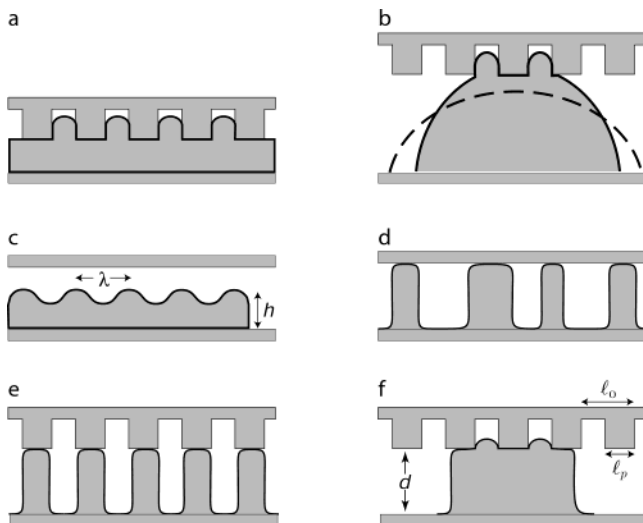


Figure 1. Schematic representation of liquid morphologies in a confined geometry: (a) embossing ($d < h$) and (b) arrested dewetting ($d \gg h$). The initial spontaneous capillary instability in part c leads to the formation of capillary bridges in part d. In the presence of the laterally varying confinement in part e, capillary bridging occurs at locations of maximal confinement. This situation does not, however, represent the lowest free energy situation shown in part f. l_p/l_o is the projection of the fraction of down-protruding surface area A_p/A_0 (eq 1).

down to 100 nm. In these experiments, the spatial confinement of the liquid was of crucial importance: only the combination of confinement and an external force leads to pattern replication.

In this context, the question arises in which way the confinement of a liquid film by itself (i.e., in the absence of externally applied potentials) influences its morphology. Is it possible to couple film instabilities with capillary effects to replicate a lateral topographic structure?

In this article, we describe the different scenarios that can take place when a polymer films dewets in a slitlike geometry (i.e., a film–air double layer placed between a planar substrate and a patterned plate, shown schematically in Figure 1).

2. Experimental Section

Our experimental system consisted of polymer films confined between two plates, one of which had a design topographic pattern. The polymer films were spin-cast from a mixture (2:5 by weight) of polystyrene (PS; molecular weight, $M_f = 106$ kg/mol, polydispersity $M_w/M_n = 1.03$) and poly(vinyl methyl ether) (PVME; $M_f = 33$ kg/mol, $M_w/M_n = 1.15$) in toluene onto silicon wafers, resulting in film thicknesses ranging from 60 to 300 nm. Prior to film deposition, all surfaces were cleaned in a jet of CO_2 expanded through a small nozzle (“snow-jet”).²⁸ The confining surface was in addition rendered apolar by the deposition of a self-assembled alkane monolayer. Dewetting was initiated by annealing the film in an oven at 170 °C for times ranging from several minutes up to 1 h. The films were analyzed by optical and atomic force microscopy (AFM) after quenching the samples to room temperature and removing the confining surface.

Films of PS/PVME mixtures on silicon wafers were chosen because such films exhibit a capillary surface instability when heated above the glass transition temperature of the mixture,²⁹ as shown in Figure 2. In contrast, pure PS and PVME films are metastable on silicon and break-up by the heterogeneous nucleation of holes.^{8,10}

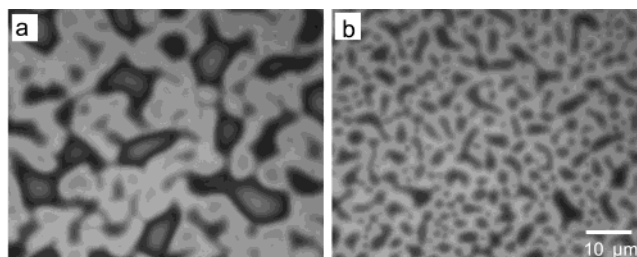


Figure 2. Onset of the film instabilities of a 110-nm-thick PS/PVME film that was heated to 170 °C for 60 s: (a) confined between two silicon wafers spaced at $d = 308$ nm and (b) no confinement. The undulatory character of the structures is due to a spontaneous surface instability in both cases. The larger amplitude of the surface undulation in part a indicates an earlier onset of the instability compared to part b, presumably due to differing initial heating rates when placing the sample in the oven. This accounts also for the more coarse grained appearance of the structure in part a due to a longer coalescence time.

The interpretation of the dewetting process of partially compatible mixtures is, however, somewhat more complex compared to homopolymer films. While miscible at low enough temperatures, PS/PVME blends demix upon heating.³⁰ The PS/PVME mixture used in this study has a lower critical point of ~ 40 °C.³¹ The data taken at 170 °C, therefore, exhibits an interplay of demixing and dewetting. While a demixing morphology on the micrometer scale takes several hours to form (much longer than the annealing times used in this study),³¹ the formation of surface enriched layers occurs much more rapidly. PVME segregates not only at the air surface,³² it also forms a layer at the substrate interface.²⁹ The formation of a thin PVME surface layer is, however, beneficial for our experiment. In the presence of such a layer, dewetting occurs at the liquid–liquid interface,³³ significantly reducing imperfections by contact-line pinning. Apart from the small interfacial segregation, the simultaneous demixing of the blend during dewetting influences the experiments only a little, and similar results are expected when using homopolymer films.

3. Results and Discussion

We start with the examination of the film instability in a laterally homogeneous slit pore. Figure 2 shows the development of a spontaneous surface instability of a 110-nm-thick PS/PVME film heated to 170 °C, (a) confined in a 308-nm-wide slit and (b) in the absence of confinement. Clearly, the film breaks up via a spontaneous undulatory instability, both in the confined geometry as well as in the unconfined case. Figure 2 also shows that the instability is not caused by a (spurious) external potential (electric field,^{23,24} temperature gradient^{25,26}). The surface undulations are, however, influenced by the confinement. The larger amplitude of the wave pattern in Figure 2a indicates a somewhat earlier onset of the instability. A difference in the onset of the instability implies a longer coarsening time,¹² accounting for the more coarse grained appearance compared to Figure 2b. The difference between parts a and b of Figure 2 is due to a superposition of two effects. First, the initial heat transfer is more rapid in the confined geometry. When the sample was put into the oven, both confining plates were brought into contact with metal pieces that were preheated to 170 °C, whereas the unconfined film was brought into good thermal contact only on the substrate side. Second, the van der Waals

(29) Morariu, M. D.; Harkema, S.; Steiner, U. Manuscript in preparation.

(30) Reich, S.; Cohen, Y. *J. Polymer Sci., Polym. Phys. Ed.* **1981**, *19*, 1255.

(31) Morariu, M. D.; Steiner, U. Submitted for publication.

(32) Cowie, J. M. G.; Devlin, B. G.; McEwen, I. J. *Polymer* **1993**, *34*, 501.

(33) Lambooy, P.; Phelan, K. C.; Haugg, O.; Krausch, G. *Phys. Rev. Lett.* **1996**, *76*, 1110.

(27) Schäffer, E.; Harkema, S.; Roerdink, M.; Blossey, R.; Steiner, U. *Adv. Mater.* **2003**, *15*, 514.

(28) Sherman, R.; Hirt, D.; Vane, R. J. *J. Vac. Sci. Technol.* **1994**, *12*, 1876.

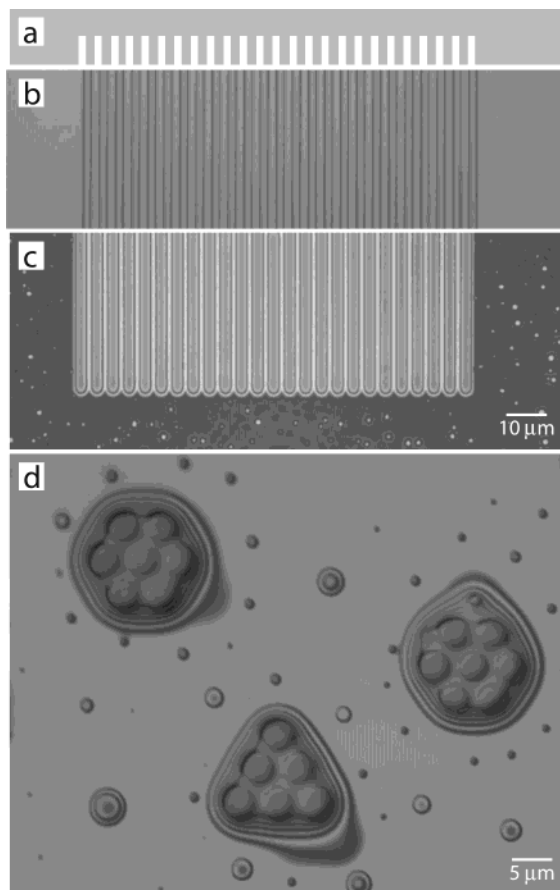


Figure 3. Extreme limits of pattern replication in a confined geometry. If $d/h < 1$, the surface protrusions are pressed into the polymer film, leading to a negative replica (embossing). The 25 lines in part c protrude from the film. They correspond to grooves in the master plate (b), with a cross section schematically shown in part a. For $d/h \approx 3.5$ ($h = 272$), drops are formed that contract to reach their equilibrium contact angle. During the associated increase in the drop height, they touch the confining surface, partially assuming its pattern in part d (see Figure 1b).

disjoining pressure is slightly increased by the confinement. In our sample geometry with $d > 3h$, however, the change in disjoining pressure is small (a few percent), leading to marginal changes of both the instability wavelength and the rupture time of the film. In the case where $d \lesssim 2h$, on the other hand, we expect an increased van der Waals disjoining pressure, induced by the confining surface.

Overall, the difference between parts a and b of Figure 2 is only small. Both films exhibit a spontaneous instability after a characteristic time of approximately 60 s, indicating that the confinement plays only a small role in this initial phase of film breakup.

After long enough times, the undulation amplitude becomes comparable to the confinement d . We subdivide our experimental results into three regimes according to the ratio of initial film thickness h and maximal confinement d (i.e., the lowest value of the interplate spacing). The limit $d/h < 1$ (Figure 1a) corresponds to the trivial situation in which the surface protrusions are pressed into the polymer, leading to the well-known embossing (or imprinting) techniques.³⁴ This is shown in Figure 3c, where a pattern consisting of 25 grooves (Figure 3a,b) was replicated by pressing it into the polymer film.

In the other limit for relatively high values of d/h , the initial instability leads to the formation of drops, whose contact angle increases until the drops attain equilibrium. During this retraction of the drops (dotted line in Figure 1b), the heights of the drops increase, reaching their maximal heights in equilibrium. If the maximal drop height is larger than d , the drops eventually touch the patterned substrate, leading to a situation schematically depicted in Figure 1b (solid line). This is shown in Figure 3d, where three large drops have locally replicated the pattern of the confining surface. The amount of filling of the confining pattern depends on its surface energy. Because an apolar confining surface was used, the pattern was only partially filled (see also ref 35). Capillary forces would, on the other hand, completely fill a high-surface-energy pattern.

More interesting is the strongly confined case of $d \gtrsim h$. Here, an initial undulation of the film (Figure 1c) leads to a bridging of the liquid between the two plates (Figure 1d). If the confining plate is patterned, these bridges form in the regions of greatest confinement, that is, at the locations where the topographic pattern of the top plate extends down toward the polymer film (Figure 1e). In this limit of d/h , we also expect the presence of weak gradients in the van der Waals disjoining pressure pointing toward the protrusions of the confining surface, aiding the pattern-replication process. In Figure 4c, the replication of a line pattern is shown. Rather than filling the 25 grooves of the confining surface in Figure 4b (cross section, Figure 4a), the 24 lines are replicated by the formation of capillary bridges; the polymer spans from the substrate to the confining surface, thereby replicating the pattern. In the nonpatterned areas, on the other hand, the polymer has coalesced to wide plugs (corresponding to the schematic drawing in Figure 1d). The difference between this mechanism and embossing can clearly be seen by comparing Figures 3c and 4c. In both cases, the same confining surface was used, resulting in 25 lines in Figure 3c (i.e., a negative replica of the confining pattern) versus 24 lines in Figure 4c (positive replica).

In a second example, the AFM images in Figure 4d,e, corresponding to the replicated polymer pattern and the confining plate, respectively, clearly show the nature of the replication process: as opposed to imprinting or replication by capillary filling (see below), where a negative replica is produced, the positive replication of the of hexagon-shaped holes on a triangular lattice clearly shows the novel nature of the replication process.

The relevant regime of d/h is determined by two conditions. (1) For capillary bridging to take place in a more or less homogeneous fashion, there has to be an approximate matching of the instability wavelength λ (see Figure 2) and the periodicity of the confining pattern.²⁹ (2) More stringently, because the polymer is nonvolatile, volume conservation applies. This implies that, per unit area A_0 , the volume of the initial film must be laterally accommodated in the replicated structure. This imposes a second condition on d/h

$$d/h \approx A_0/A_p \quad (1)$$

where A_p is the lateral area of the protrusions of the confining surface extending down toward the polymer film (Figure 1). The first condition has to be fulfilled within 1 order of magnitude, but the second condition also allows

(34) Xia, Y.; Rogers, J. A.; Paul, K. E.; Whitesides, G. M. *Chem. Rev.* **1999**, *99*, 1823.

(35) Blossey, R. *Nat. Mater.* **2002**, *2*, 301.

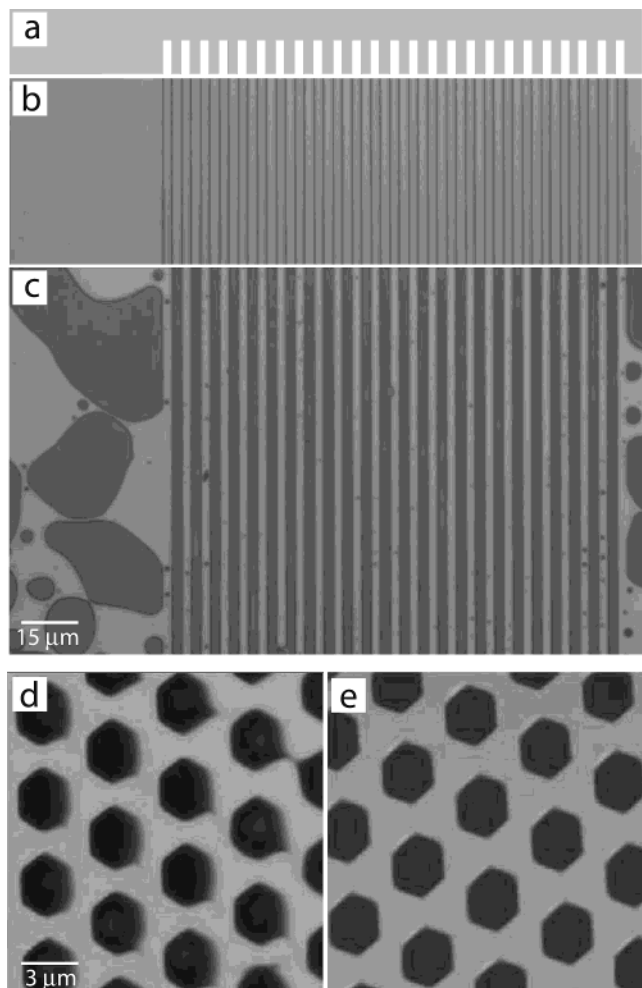


Figure 4. Dewetting in a confined geometry. The 24 replicated lines in part c correspond to the 24 downward protruding lines of the master shown in part b. These lines were replicated into the polymer film by capillary bridging ($d/h = 1.4$, $h = 84$ nm). A schematic cross section of the confining surface is shown in part a. (d) An AFM image of a replicated polymer film, made with the confining surface shown in part e. The positive replica is indicative of replication by capillary bridging.

some variation because a certain degree of lateral under- or overfilling of the pattern is permissible. For $d/h \ll A_0/A_p$, the material that cannot be accommodated in the locations of greatest confinement gives rise to defects in the replication (e.g., plugs between the lines, not shown). In the opposite limit ($d/h \gg A_0/A_p$), the confining pattern is only incompletely replicated (Figure 5).

The reproduced polymer patterns in Figure 4c,d clearly do not represent the equilibrium pattern of the liquid inside the slit. This becomes clear when comparing the liquid morphologies schematically shown in Figure 1e,f. The filled morphology in Figure 1f has a much lower polymer–air surface area and, therefore, a reduced overall surface energy. It is, therefore, expected that all the patterns shown in Figure 4 must undergo a filling transition after long enough times.

In Figure 5, only the partial replication of a hole pattern was achieved. Most of this image shows patches, where the pattern of the confining surface (a hexagonal array of holes) was replicated. Because this sample had a value of $d/h = 2.5$, which was larger than $A_0/A_p = 2$, there was insufficient material in the film to fully replicate the confining surface, leading to the patched appearance of the polymer pattern. An interesting additional feature in

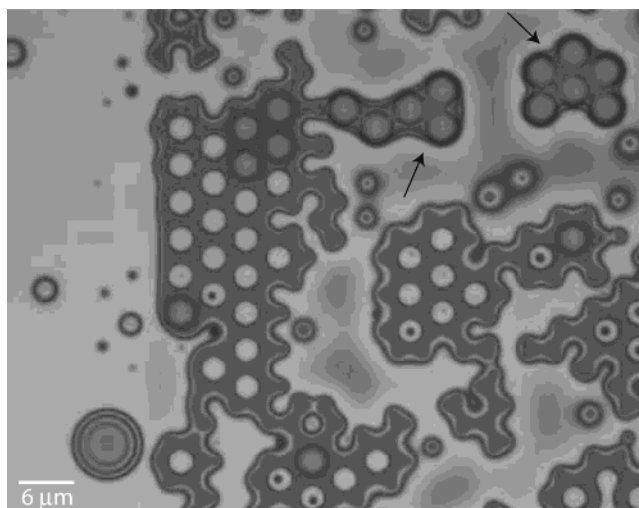


Figure 5. Imperfect replication of the hexagonal pattern of holes ($d/h = 2.5$, $h = 110$ nm) shows the onset of a filling transition. In some of the smaller replicated areas, the polymer has filled the hole pattern (marked by arrows), which still persists on the remaining parts of the sample.

Figure 5 is pointed out by the arrows. In these regions, the patterned slit pore was partially filled, with a morphology consisting of cylindrical columns surrounded by a polymer film. We postulate that this is the onset of a filling transition, that is, the transition from part e to part f of Figure 1. Because such a filling transition involves a lateral contraction of the substrate area wetted by the polymer (compare parts e and f of Figure 1), which necessitates the motion of all contact lines, this transition is expected to proceed more rapidly for the smaller patterned regions (arrows in Figure 5), compared to larger replicated areas.

Therefore, the lifetime of the positive replicas shown in Figure 4 is enhanced by the large number of contact lines, both on the substrate and on the confining surface. The filling transition (part e to part f of Figure 1) requires a lateral motion of all contact lines, a process that is known to be very slow.³⁶ The suppression of lateral coalescence can also be seen in Figure 4c. While the polymer in the nonstructured region left of the line pattern has coalesced to large plug-shaped drops, the coarsening of the polymer in the patterned gap was suppressed by the pinning of the polymer on the edges of the protrusions of the confining surface.

A precondition for the successful pattern replication is the correct choice of boundary conditions. The apolar nature of the confining surface is essential to obtain a positive replication of the patterned surface. Highly apolar surfaces are typically not wetted by any liquid because the coating of the surface by the liquid does not reduce its effective surface energy. Corrugated apolar surfaces repel any type of surface coverage to a very large extent.³⁵ Such surfaces are, therefore, often termed superhydrophobic or self-cleaning. In Figure 4, capillary forces that drive the polymeric liquid to completely fill the surface pattern are absent. This enables the formation of the metastable morphologies corresponding to Figure 1e.

If, on the other hand, a more polar confining surface is used, capillary forces drive a rapid and complete filling of the patterned surface. An example of this effect is shown in Figure 6, where the self-assembled monolayer on the confining surface was imperfect. The polymer in contact

(36) Léger, L.; Joanny, J. F. *Rep. Prog. Phys.* **1992**, *55*, 431.

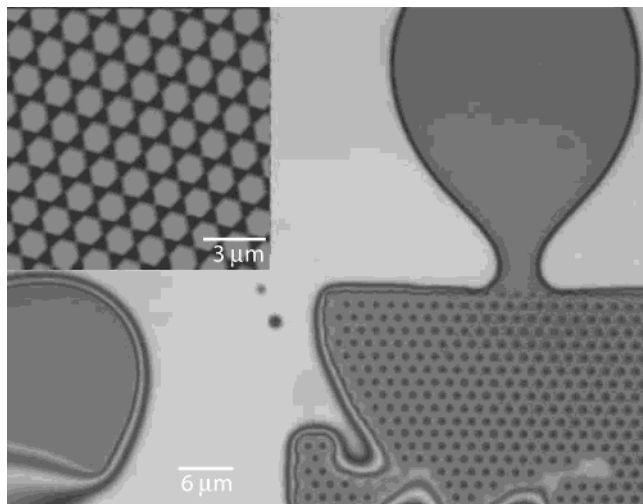


Figure 6. Capillary filling of a patterned slit. If the confining surface is polar, capillary forces draw the polymer toward the regions of highest confinement. This way, a drop in contact with a pattern is drawn into the patterned slit ($d/h = 4.3$, $h = 103$ nm). The inset shows an AFM image of the confining surface.

with the surface pattern (possibly part of the drop in Figure 6, top right) was drawn into the patterned slit pore, completely filling its topographic pattern. As opposed to the images in Figure 4, the patterned polymer film shown in Figure 6 is a negative replica of the confining surface. This effect, the capillary filling of a patterned high surface energy surface, is a well-known alternative structure-replication technique.^{34,37}

4. Conclusion

In summary, our study of dewetting in a patterned confinement shows a rich variation of replication mechanisms. While the well-known embossing and capillary-filling techniques result in a negative replica of a surface pattern, a novel phenomenon was observed for a confinement with $d \gtrsim h$. In this case, metastable liquid morphologies are formed by the interplay of dewetting and capillary bridging. The lateral formation of the capillary bridges can be controlled and directed using a patterned confining surface. This, combined with the pinning of a large number of contact lines, leads to a long-lived, metastable positive replica of the confining surface.

Interestingly, a single experimental system consisting of a polymer film and a topographically patterned plate can be used in three different ways in a replication technique: (1) embossing, (2) capillary filling, and (3) capillary bridging, with 1 and 2 resulting in negative replica and 3 resulting in a positive replication process. The combination of these three techniques exhibits a versatility not normally found in similar pattern-replication processes.

Acknowledgment. We thank B. Maile and eXtreme Lithography for the master patterns. This work was partially funded by the Dutch “Stichting voor Fundamenteel Onderzoek der Materie” (FOM) and the Dutch Polymer Institute (DPI).

LA034527B

(37) Suh, K. Y.; Lee, H. H. *Adv. Funct. Mater.* **2002**, *12*, 405.